Study of Electrical and Magnetic Properties of Cerium Doped Nano Smart Magnesium Ferrite Material

K.Muthuraman
Dept of Chemistry
Sethu Inst. of Tech.,
Pulloor – 626115,
Tamilnadu, India

Vasant Naidu
Professor/ECE
Sethu Inst. of Tech.,
Pulloor – 626115,
Tamilnadu, India

S.K.A.Ahamed. Kandu Sahib
Asso. Prof / ECE
Sethu Inst. of Tech.,
Pulloor – 626115,
Tamilnadu, India

T.Vasudevan
Former Professor
Dept of Industrial chemistry
Alaggappa University
Karaikudi – 630003,
Tamilnadu, India

ABSTRACT

Nano Smart Magnesium Cerium ferrite material had been synthesized by sol-gel route. The crystalline structure and grain size of these particles were analyzed by using XRD, the particle size ranged from 46.61nm to 82.12 nm. The decrease in value of the lattice parameter with doping suggests that the shrinkage in unit cell and the crystallite size increase with Ce^{3+} concentration. The SEM and EDAX studies helped in confirming the presence of elements and the size of the material particles. The permittivity, dielectric loss, capacitance and inductance of these four ferrite samples with different concentration of cerium were studied within the frequency range of 2.4 to 4 GHz.. The Magnetic measurements revealed through hysteresis suggests the B-site substitution of Ce^{3+} ions in the series $MgCe_xFe_{2-x}O_4$. The variation of magnetic parameters with doping concentration is explained with the help of particle size dependence**.** Piezo properties confirmed the smart behaviour of the material.

Keywords: Magnesium cerium ferrite, nanostructure, microwave sintering, dielectric studies, Sol-Gel route, Smart material.

1. INTRODUCTION

The high resistivity and low eddy current losses of ferrite materials have been a subject of great interest in diverse technological field . These ferrites show the typical spinel ferrite structure MFeO, M represents a divalent metal ion, such as (Ni,Mn,Mg,etc..) they have a great potential for several applications due to their interesting structural, electrical, magnetic, optical properties. These materials have a wide applications as magnetic recording media, drug delivery, sensors, catalysts[1-2] etc., among the ferrites, the spinel type ferrites are particularly important since they can be used as electromagnetic wave absorbers or electromagnetic interference (EMI) suppressors in the MHz frequency range like the TV ghost suppressor [3-4] Ferrites are also used in camouflaging military aircrafts and missiles against radar detection. Among the spinel type ferrites, Magnesium cerium ferrite is a suitable material for microwave applications [5-6].

The Microwave behaviour of Magnesium (Mg) Cerium (Ce) ferrite (Fe_2O_4) prepared by sol–gel route was reported by [7]. As far as the authors know, studies on size dependent microwave properties of nanoparticles of Magnesium cerium ferrite have not been reported. The properties of are interesting due to the presence of very large and highly disordered grain boundaries. Because of the peculiarities of the grain boundaries, nano materials exhibit enhanced dielectric properties. In the present article, we report the preparation and study of microwave dielectric properties of consolidated nanoparticles of Magnesium cerium ferrite having average grain sizes ranging from 46.61 to 82.12 nm in the S band frequency range (2.4 to 4 GHz.). These properties are compared with those of sintered pellets of nanoparticles of nickel ferrite. The microwave properties like dielectric constant, dielectric loss are investigated.

The nanocrystalline ferrites can be prepared by different techniques. Number of chemical methods was developed to prepare nanocrystalline spinel ferrites. The methods include wet chemical co-precipitation [7], microwave refluxing [8], sol-gel [9], hydrothermal [10], glass crystallization, salt melt technique [11] etc. Processing of ferrites has gained tremendous importance in recent times to meet the high performance demands on ferrites in keeping pace with the vast emerging technologies. Thus the quality of ferrite powders has strong influence on the performance of final device.

The purpose of the present work is to prepare the nano sized Ce doped Magnesium ferrite and to study its structural property. Further the studies are extended for the determination of dielectric constant, dielectric loss and magnetic properties. These studies will be used for practical applications particularly for the patch antenna design and construction.

2. EXPERIMENTAL PROCEDURE

2.1 Synthesis Technique:

The nano sized Magnesium ferrite doped with different concentration of Cerium(Ce) was prepared by using the AR grade of Magnesium nitrate[$Mg(NO_3)_2.H_2O$] Lobo Chem., and Ferric Nitrate [$Fe(NO_3)_3.9H_2O$]Merck and rare earth Cerium Nitrate [$Ce(NO_3)_2.H_2O$] Alfa Aesar, along with Citric acid [$C_6H_8O_7.H_2O$] Merck in a certain molar ratio of 1:1 and weighed salts are dissolved in deionized water, here the metal ions to get segregated from the solutions with the help of citric acid for the homogenous distribution. Further a required amount of ammonia was added in order to adjust the pH value to about 7, since the base catalysts were employed in order to speed up the reaction. The solution was later subjected to a continuous stirring for duration of 24 hrs. The as prepared solution was heated to a constant temperature of 135°C to condense it into a xerogel [12]. After this dehydration process a brown colored dried gel is

obtained. The as burnt powder is further crushed in agate mortar to obtain the nano sized powder. Further the powder is subjected to sintering in a microwave furnace for a soaking duration of 30 minutes at 1250°C. By using the Scherrer's equation grain size of the nanoferrite material was determined from the prominent peak of XRD. Using the knowledge of site preference of the ions and the ionic size data, the cation distribution has been calculated theoretically, using the formula as proposed [13]. These nano ferrites possesses a very well defined local atomic ordering that may be described in terms of a spinel-type structure with Mg^{2+} and Fe^{3+} ions almost randomly distributed over its tetrahedral and octahedral sites. The new structural information helps to explain the material's enhanced magnetic properties [14]. The experimental magnetic moment was calculated from the following formula.

$$\eta = \frac{[M_W * M_S]}{5585}$$

Where Ms is the saturation magnetization in emu/g and M_W is the molecular weight.

2.2 XRD and EDAX Studies

The phase composition of fine ferrite powder was carried out using PAN analytical X'pert PRO diffraction meter using Cu K_α radiation (λ=1.54°A) at 40KV and 30mA with a scanning rate of 0.01°/s and scan speed of 1°/min in a 2θ range of 10-80°A. The crystallite size was calculated from Fig.2,3 by taking FWHM of the (311) peak in XRD and using the Scherrer formula, thus confirming the presence of Mg ferrite and the peak (333) confirms the doping of Ce Fig.1. The energy dispersive studies (EDAX) were done on Genesis EDAX to confirm the presence of chemical composition present in the powder .

2.3 FTIR Analysis

From Fig.8, the Infrared absorption spectra were found to be in the range of 3.6452 $\times 10^4$ m^{-1} to 5.6896 $\times 10^4$ m^{-1}, they were recorded at room temperature by using SHIMADZU FTIR spectrum using KBr pellet method. From the FTIR studies with respect to the spectrum transmittance (%) against wave number (m^{-1}) is used for interpretation of the results.

2.4 SEM Studies

SEM Micrographs of the nanoferrite powder were recorded using the scanning electron microscope (HITACHI model S-3000H) shown in Fig 4-7

2.5 Magnetic Measurements

The Magnetic measurements were performed on the commercial vibrating sample magnetometer (VSM) Lakeshore (Model 73009). The Magnetic hysteresis loops were measured at the room temperature with maximal applied magnetic fields up to 0.95T. Magnetic field sweep rate was kept at 5 Oe/s for all the measurements, so that the measurement of hysteresis loops with maximum field of 0.989 T was taken from an interval of three hours. The saturation magnetization, coercivity and remanent magnetization were found from hysteresis loop.

2.6 Electrical Measurements

The Electrical measurements were performed using the N4L LCR meter. The experimental set up for measuring the dielectric properties in the microwave region consists of a pellet holder connected to the N4L LCR meter interfacing the computer. The microwave properties of the four samples Ce(x) doped magnesium ferrite where x =0.01, 0.012, 0.014, 0.016 had been investigated at the frequency range from 2.4 to 4 GHz. The electrical conduction mechanism can be explained by the electron hopping model of Heikes and Johnston [15].

$$Fe^{2+} \leftrightarrow Fe^{+3} + e \text{ (or) } Mg^{2+} \leftrightarrow Mg^{3+} + e$$

3.0 RESULT AND DISCUSSION:

3.1 X-Ray Diffraction

The analysis of the XRD patterns was done and used to determine the respective planes of the face centered cubic structure of the ferrites. The well resolved peaks in XRD pattern clearly indicated the single phase and polycrystalline nature of these samples.

Figure 1 shows XRD patterns of the Mg Ce_x Fe_{2-x} O_4 sample. The diffraction patterns and relative intensities of all diffraction peaks are matched well with those of JCPDS card 22-1086 for Mg Ce_x Fe_{2-x} O_4 and the Ce diffraction peaks matched well with those of JCPDS card 34-0394. The peaks appeared at around 28°, 33.555°, 42.47°, 56.535° , 59.087° and 69.402° for Mg and Ce. These peaks were well indexed to the crystal plane of spinel ferrite (220), (311), (400), (422) (333),(440), and respectively. The figure confirms that the diffraction peaks were sharp because of the micrometer size of the crystallite. The single-phase cubic spinel structure was clearly indicated by the XRD patterns of these pure $MgFe_2O_4$. The patterns also show that all the samples had formed the cubic single spinel phase. There absence of foreign impurities was confirmed from these XRD patterns. The lattice parameter a (A°) was determined using Bragg's law.

$$a = d_{hkl}\sqrt{h^2 + k^2 + l^2}$$

here h, k, l are the indices of mentioned planes. The lattice constants for all samples prepared in investigation are listed in Table 1. It was also seen that the lattice constants of individual phases did not show a large variation by the inclusion of Cerium. The crystal size was evaluated by measuring the FWHM of the most intense peak (311) from XRD figure. The size of the crystal was determined by using the Debye Scherrer's formula [16] , given as

$$D = \frac{0.94\lambda}{\beta \cos\theta}$$

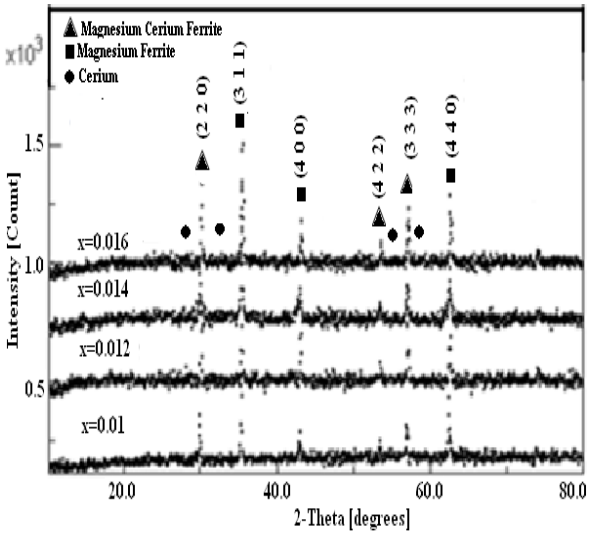

Fig1 XRD patterns of sintered Mg Ce_x $Fe_{2-x}O_4$ x=0.01, 0.012, 0.016, 0.018

Table 1 XRD cation distribution of $MgCe_x$ $Fe_{2-x}O_4$

Sample x	Lattice Constant (A°)	Particle size(nm)
0.01	8.3732	51.113
0.012	8.39	82.12
0.014	8.4076	46.61
0.016	8.371	67.22

Further the XRD patterns shows the narrow reflections were exhibited due to the narrow size crystallites. The mean crystallite size of the sample lies within the range of 46.61nm to 82.12nm. The lattice parameter shows an increases up to x = 0.014 composition and then starts decreasing for 0.016 composition.

3.2 EDAX

The EDAX spectra (Fig.2 and Fig 3) obtained from the center of Ce substituted Mg ferrite grains indicated the presence of Mg peaks at 1.8 – 1.9.keV, where as Ce grains are seen in between the energy range of 4keV and 6.5keV where as the Fe peaks are seen at 6.2keV and 6.8keV.

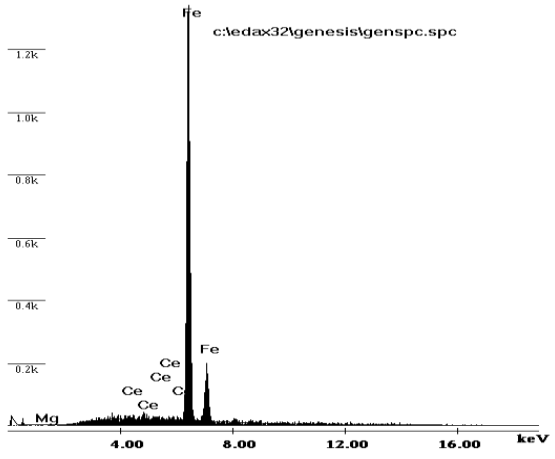

Fig 2 EDAX pattern for Mg Ce_x $Fe_{2-x}O_4$ x=0.012

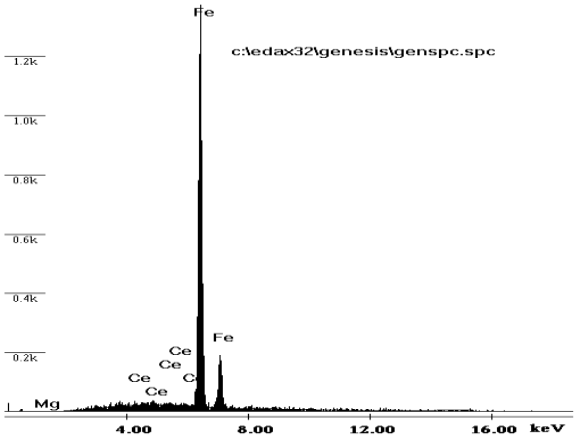

Fig 3 EDAX pattern for Mg Ce_x $Fe_{2-x}O_4$ x=0.014

3.3 SEM analysis

The SEM micrograph confirms the nano phase of the crystallite shown in Fig. 4-7. The analysis confirmed the microstructure of the sintered specimen. The Ce-doped specimens show a bi-phasic microstructure that is formed of dark ferrite matrix grains with small whitish grain at the grain boundary. As proposed by Sattar et, al [17] the grain boundaries or the iron positions are occupied by the rare earth ions. The probability that the rare earth ions will occupy the A site of Fe^{3+} ions are excluded. And this is due to the fact that the tetrahedral sites are small to be occupied by the large rare earth ions which have large ionic radius. Also the probability of occupancy of the octahedral (B-site) is by the rare earth ions (Ce). With the increase in doping ions concentration the ionic radius R decreases. This is indicated in the whitish grains of Ce with Fe_2O_4.

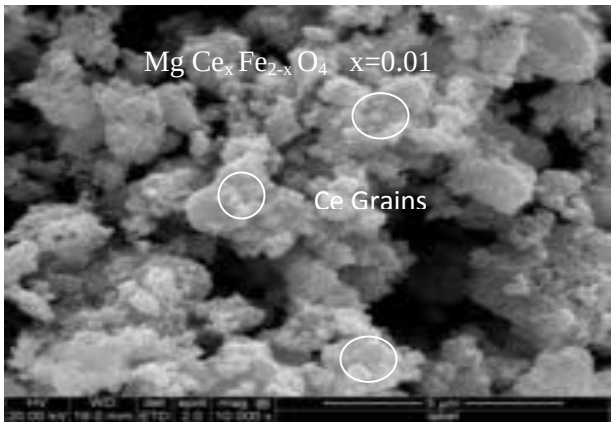

Fig.4 $MgCe_xFe_{2-x}O_4$ x=0.01

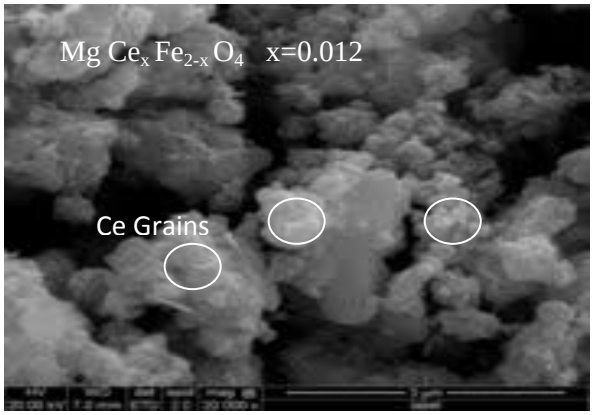

Fig.5 $MgCe_xFe_{2-x}O_4$ x=0.012

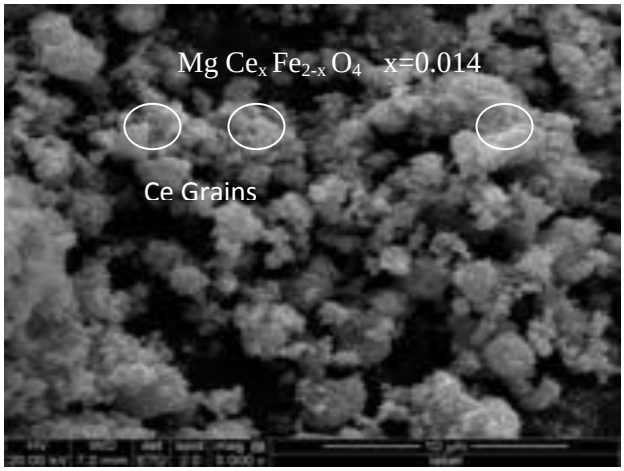

Fig.6 $MgCe_xFe_{2-x}O_4$ x=0.014

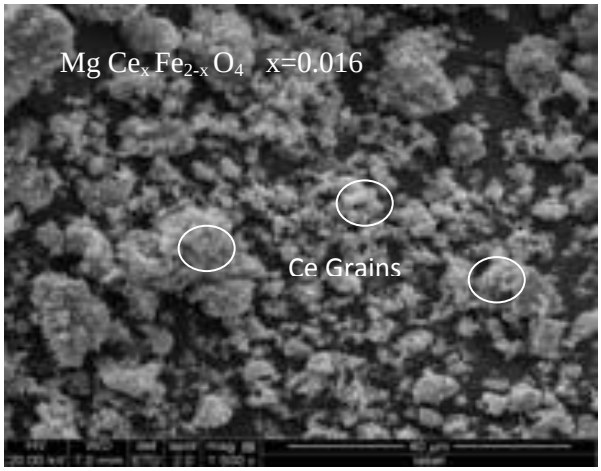

Fig.7 $MgCe_xFe_{2-x}O_4$ x=0.016

The amount of Ce with Fe $_2O_4$ was maximum in x = 0.01 composition. The grain size of matrix phase was also maximum for x = 0.016 composition. Relatively lower grain size of ferrite matrix was seen in x= 0.012 compositions, it may be due to the grain growth inhibition caused by the change in percentage composition of Ce in Ce Fe $_2O_4$.

3.4. FTIR study

The far-infrared spectra study is an important tool to obtain the information about the ion position in the crystal [18]. FTIR absorption spectra of the samples at high and low frequency absorption bands (υ_1,υ_2) lies in the range from 5.6896×10^4 m^{-1} to 3.6452×10^4 m^{-1} are tabulated in Fig. 8. The two major absorption bands mentioned in Table 2 shows the spectra in the frequency range, which attributes to the tetrahedral and octahedral complexes Fe^{3+}–O^{2-} Waldron [19] reported the two bands were by in spinel structure of ferrite, the shift of absorption band υ_1 and υ_2 had been observed. With the addition of R ions the absorption band υ_1 and υ_2 are slightly shifted to upper frequency side and this attributed to increase in bond length on the B-site [20]. This exhibits that the rare-earth ions occupy the B-site. The difference between the frequencies υ_1 and υ_2 are due to changes in bond length (Fe^{3+}–O^{2-}) at tetrahedral and octahedral sites.

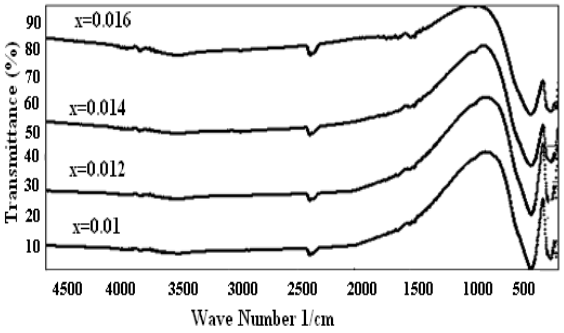

Fig 8 FTIR absorption spectra of the sample Mg Ce_x $Fe_{2-x}O_4$

The broadening of the υ_2 band is observed when rare-earth element is added $MgFe_2O_4$, which suggests the occupancy of rare-earth ions on the B-sites [21].The inter-ionic separation may face an extension owing to less number of structural matters in the surrounding of each nano particle. Hence the nano size of the ferrite particles and ultimate change of the nature of ions in the respective size could have caused reduction of magnetization in $MgFe_2O_4$. Thus in the nano regime, the magnetization is said to be dependent on the grain size and cation distribution. Table 2 shows the changes observed due to the change in doping concentration of Cerium., here υ_1 and υ_2, increases. The graphs confirm these results regarding the stability, which

increases for the substituted samples and are homogeneous under the decreased stress conditions.

Nano Composite $MgCe_XFe_{2-x}O_4$	Absorption/Cm^{-1}	
	υ_1	υ_2
X=0.01	565.1	364.52
X=0.012	565.1	366.45
X=0.014	567.03	366.45
X=0.016	568.96	366.45

Table 2 FTIR to show the rare-earth ions occupation

3.5 Hysteresis studies

The different parameters such as saturation magnetization (M_C), coercive force (H_C), and Retentivity, The dielectric constant ε_r and dielectric loss ε_r' are listed in Table 3. The magnetic properties have been seen to be altered by the addition of Ce in Mg ferrite, It was observed that the saturation magnetization increases with the addition of Ce. Rezlescu et al. [22], the saturation magnetization of Ce^{3+} substituted Mg ferrites is higher than that of unsubstituted ferrite. Fig.9 shows the variations in saturation magnetization (M_S) for the different x values of nano composite $MgCe_xFe_{2-x}O_4$, the saturation magnetization (M_S) value increases with the increase in value of x. This is due to the increasing of Cerium content, which induced a phase transition from polar-to-non polar region. A rhombohedral and two orthorhombic modifications within the polar region of $MgCe_xFe_{2-x}O_4$ were found. It is also seen that the Cerium substitution resulted in the appearance of spontaneous magnetization, which was significantly enhanced upon the composition-driven transition from a rhombohedral to an orthorhombic phase.

The coercive force show linear decrease initially and later shows a gradual increase with the increase in the doping concentration. M_S, H_C, M_R the magnetic parameters of nano particles of $MgCe_xFe_{2-x}O_4$ were obtained from the VSM data. Through the cation distribution the difference in the value of M_S can be explained.

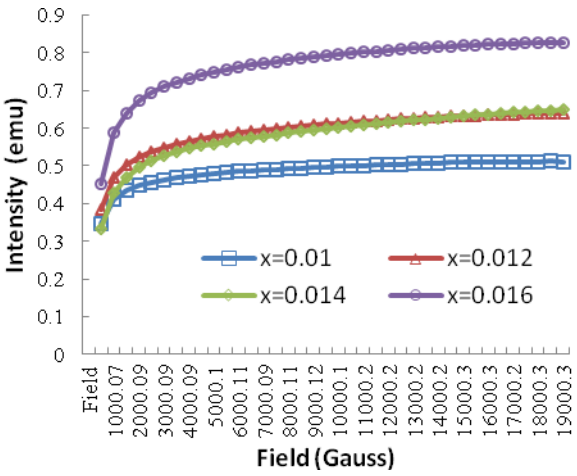

Fig 9 Saturation magnetization (Ms) for Mg Ce_x $Fe_{2-x}O_4$

Any change in the concentration and nature of the ions in A and B site should cause resultant magnetization to be different as reported.

Table 3 Magnetic saturation, of Mg Ce_x $Fe_{2-x}O_4$

Mg Ce_x Fe_{2-x} O_4 X	Magnetic Saturation (emu)	Coercivity	Retentivity	ε_r	ε_r'
0.001	0.51660	140.86	0.13650	3.8	4.37
0.012	0.64289	134.46	0.14146	2.69	3.00
0.016	0.65246	94.586	0.0775	0.645	0.562
0.018	0.83079	144.40	0.18184	2.254	2.323

3.6 Electrical Studies:

The dielectric constant ε_r and dielectric loss $\varepsilon_{r'}$ of the sintered samples $MgCe_xFe_{2-x}O_4$ over the microwave frequency range from 10M Hz –20GHz are shown in figure 10 and 11. The plots 10,11 show that the ε_r and ε_r' values tend to decrease exponentially, it is also seen that the value of ε_r and ε_r'increases with the addition of the Cerium concentration, while the capacitance value remains fairly constant over the frequency range of study,. The maximum value of dielectric constant 3.8 is observed for the sample $MgCe_{0.01}Fe_{1.99}O_4$ and minimum is 0.645 for the sample $MgCe_{0.016}Fe_{1.86}O_4$, as mentioned in Table 3.

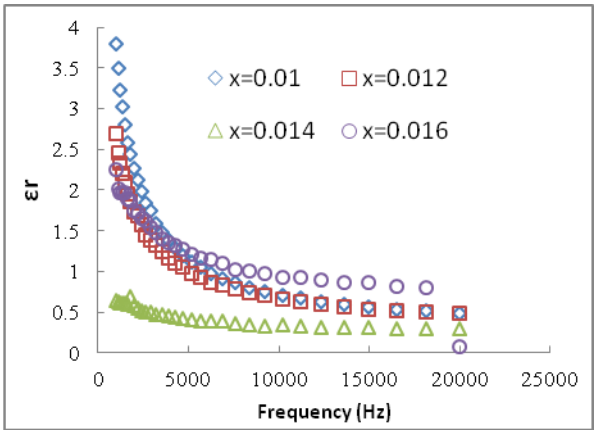

Fig.10 Dielectric constant (ε_r) for Mg $Ce_xFe_{2-x}O_4$ in the B-site

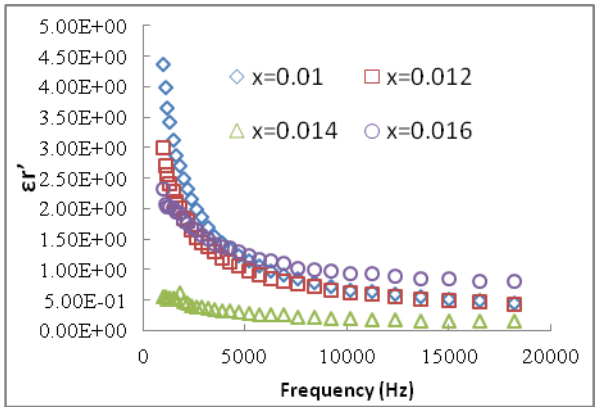

Fig.11 Dielectric loss(ε_r') for Mg Ce_xFe_{2-x} O_4

3.6 Piezo Electric Study

In these study it was found that with the increasing load increase in voltage been seen shown in Fig.12. This conforms the piezo electric behaviour of this material. This concludes the smart behaviour of these ceramic materials(23,24).

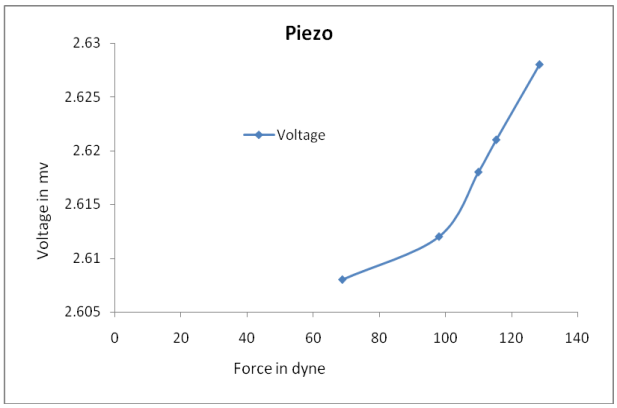

Fig.12 Piezo electric study

4. Conclusion:

The sintered powder of magnesium Cerium ferrites produced by sol gel route and for this grounded powder the following correlations were observed between microstructure , magnetic properties and electrical properties. It is clearly evident from the above experimental results, that the nano size of the ferrite particles has caused increase in magnetization in Ce doped $MgFe_2O_4$. Since Saturation magnetization and coercive force increases with the increase in Ce concentration. The saturation magnetization of this powder was determined using a Vibrating Sample Magnetometer (measured at LAKESHORE VSM model 73009). Hysteresis losses, maximum magnetization and magnetic remanance showed a minimal change. There was no substantial change in the coercive force as expected; therefore doping percentage has to be increased. The effect of substituting magnesium with Cerium in magnesium cerium ferrites on the magnetization of magnesium ferrite differs significantly from that promoted by replacing iron with cerium, probably due to differences in the ratio of the cationic radii of the coupling nonferrous elements. The Piezo behaviour of these material, confirms their smart effects, therefore these studies have the practical importance to design the antenna. This change will be also suitable for reducing the size of the antenna. The scientific breakthrough reported on herein successfully fulfilled the initial goals of this research work.

5. REFERENCES

[1] Mahindrakar Rohini, Algude S.G. and Birajdar D.S Electrical and dielectric properties of Zirconium doped Nickel-Zinc ferrite, Journal of Physics, ISSN: 0976–7673 & E-ISSN: 0976–7681, Vol. 1, Issue 1, 2010, PP-14-19.

[2] Rao B. P., Rao K. H., rao A. P., Rao T. V., pandarua.and Caltun O. F. 2005 J. Optoelectron. Adv. Mater. 7 701.

[3] Gopal Reddy C V, Manorama S V and Rao V J 1999 Sensors and Actuators B55 90

[4] Luo H Y, Yue Z X and Zhou J 2000 J. Magn. Magn. Mater. 210 104

[5] Meshram M R et al 2002 Bull. Mater. Sci. 25 169.

[6] Muthuraman et.al., Synthesis of Nano sized Ce-Co Doped Zinc Ferrite and their Permittivity and Hysteresis Studies. International Journal of Computer Applications (0975 – 8887) Volume 32– No.3, October 2011.

[7] Vasant Naidu, S.K.A.Ahamed Kandu Sahib, M.Suganthi, ChandraPrakash; Study of Electrical and Magnetic properties in Nano sized Ce-Gd Doped Magnesium Ferrite, International Journal of Computer Applications vol 27, 5(40-45) 2011

[8] Vasant Naidu, S.Vijayaragavan, R.Legadevi, A.Senthil kumar Synthesis of Nano sized Sm-Gd doped Magnesium ferrite and their Permittivity and Hysteresis Studies, International Journal of Computer Applications vol 30(7), (13-23) 2011

[9] Jadhav, Inter. J. Mod. Phys. B 23 (2009) 5629.

[10] Jyotsendu Giri, Sriharsha T., Bhadur D., J. Mater. Chem. 14 (2004) 875.

[11] Sato H., Hameda T., IEEE Magn. Trans. 34 (1993) 76.

[12] Simon Thompson, Neil J. Shirtcliffe, Eoins O'Keefe, Steve Appleton,

[13] Jiangno Huang, Hanrui Zhnang, Wen Lan Li, J. Mater. Res. Bull. 38 (2003) 149.

[14] F. Mansour "Frequency and Composition Dependence on the Dielectric Properties for Mg-Zn Ferrite". Egypt. J. Solids, Vol. (28), No. (2), (2005)

[15] R. R. Heikes and D. Johnston, The Preparation and Magnetic Properties of High Purity Raney Iron J. Chem. Phys. 26, 582 (1957).

[16] Cullity B.D., Elements of X-Ray Diffraction, Addison Wesley Pub. Co. Inc., London 1967: 96.

[17] A.A Sattar.., et.al, Rare Earth Doping Effect on the Electrical Properties of Cu-Zn Ferrites, [J] J. Phys. IV France 1997, 7.

[18] Gadkari A.B., Shinde T.J., and Vasambekar P.N., Structural analysis of Y^{3+} doped Mg-Cd ferrites prepared by oxalate co-precipitation method, J. Mater. Chem. Phys., 2009, 114 (2-3): 505.

[19] Waldron R.D., Infrared spectroscopy of ferrites, Phy. Rev., 1955, 99: 1727.

[20] Hemeda O.M., IR spectral studies of $Co_{0.6}Zn_{0.4}Mn_xFe_{2-x}O_4$ ferrites, J. Magn. Magn. Mater., 2006, 281: 36.

[21] Vasant Naidu, S.K.A.Ahamed Kandu Sahib, M.Sheik Dawood, M.Suganthi; Magnetic Properties of Nano Crystalline Nickel, Cerium doped Zinc Ferrite , International Journal of Nano tech and Nano Sci in press.

[22] N Rezlescu., ERezlescu., C Pasnicu., and M.L Craus., Effect of the rare-earth ions on some properties of nickel-zinc ferrite, J. Phys. Condens. Matter, 1994, 6: 5707.

[23] Manbachi, A. and Cobbold R.S.C. (2011). "Development and Application of Piezoelectric Materials for Ultrasound Generation and Detection". Ultrasound 19 (4): 187–196

[24] S. Trolier-McKinstry (2008). "Chapter3: Crystal Chemistry of Piezoelectric Materials". In A. Safari, E.K. Akdo˘gan. Piezoelectric and Acoustic Materials for Transducer Applications. New York: Springer. ISBN 978-0-387-76538-9.